Structural, MALDI-TOF-MS, Magnetic and Spectroscopic Studies of New Dinuclear Copper(ii), Cobalt(ii) and Zinc(ii) Complexes Containing a Biomimicking μ-OH bridge

ARTICLE *in* DALTON TRANSACTIONS · NOVEMBER 2010

Impact Factor: 4.2 · DOI: 10.1039/c0dt00692k · Source: PubMed

10 AUTHORS, INCLUDING:

Cristina Nuñez
New University of Lisbon
55 PUBLICATIONS **416** CITATIONS
SEE PROFILE

Pablo J González
Universidad Nacional del Litoral
33 PUBLICATIONS **532** CITATIONS
SEE PROFILE

Jose Luis Capelo
New University of Lisbon
188 PUBLICATIONS **2,405** CITATIONS
SEE PROFILE

Carlos Lodeiro
University NOVA of Lisbon
239 PUBLICATIONS **3,006** CITATIONS
SEE PROFILE

Structural, MALDI-TOF-MS, Magnetic and Spectroscopic Studies of New Dinuclear Copper(II), Cobalt(II) and Zinc(II) Complexes Containing a Biomimicking μ-OH bridge†

Cristina Núñez,[a,d] Rufina Bastida,*[a] Alejandro Macías,[a] Laura Valencia,[b] Nicolás I. Neuman,[c] Alberto C. Rizzi,[c] Carlos D. Brondino,*[c] Pablo J. González,[d] José Luis Capelo[d,e] and Carlos Lodeiro*[d,e]

Received 21st June 2010, Accepted 17th September 2010
DOI: 10.1039/c0dt00692k

The $Py_2N_4S_2$ octadentate coordinating ligand afforded dinuclear cobalt, copper and zinc complexes and the corresponding mixed metal compounds. The overall geometry and bonding modes have been deduced on the basis of elemental analysis data, MALDI-TOF-MS, IR, UV-vis and EPR spectroscopies, single-crystal X-Ray diffraction, conductivity and magnetic susceptibility measurements. In the copper and zinc complexes, a μ-hydroxo bridge links the two metal ions. In both cases, the coordination geometry is distorted octahedral. Magnetic and EPR data reveal weakly antiferromagnetic high spin Co(II) ions, compatible with a dinuclear structure. The magnetic characterization of the dinuclear Cu(II) compound indicates a ferromagnetically coupled dimer with weak antiferromagnetic intermolecular interactions. The intra-dimer ferromagnetic behaviour was unexpected for a Cu(II) dimer with such μ-hydroxo bridging topology. We discuss the influence on the magnetic properties of non-covalent interactions between the bridging moiety and the lattice free water molecules.

Introduction

Dinuclear copper, zinc and cobalt model complexes have been extensively studied because of their relevance to understanding the properties of the bimetallic centres present in several metalloenzymes and metalloproteins.[1] Copper catechol oxidase and tyrosinase, cobalt methionine aminopeptidase and a huge number of zinc hydrolases are prototypical examples of enzymes containing dinuclear metal centres.[2,3] The crystallographic structure of native catechol oxidase from sweet potatoes (*Ipomoea batatas*) has shown that this enzyme contains a dinuclear copper site with three histidine ligands per copper atom and an additional hydroxyl group bridging the metal ions.[4]

In the state identified as "met",[5] the copper atoms lie 2.9 Å apart and are antiferromagnetically coupled ($-2J > 600$ cm^{-1}), which is characteristic for type-3 copper sites.[6] Another example of a dinuclear Cu centre is the active site of the enzyme tyrosinase, which is an enzyme present in animal tissues and plants that catalyzes the production of pigments such as melanin and others by the oxidation of tyrosine. The active site of tyrosinase presents two copper atoms, each coordinated by three histidine sidechains and with a μ-hydroxo bridge between the copper ions.[7]

On the other hand, a dinuclear cobalt site can be found in the metalloprotease methionine aminopeptidase, an enzyme involved in angiogenesis and the development of various forms of cancer in humans.[8] The active site of these enzymes comprises two cobalt ions 2.9 Å apart.[9] The Co(II) metal ions are linked by the side chains from several amino acids. The determination of the crystallographic structure of methionine aminopeptidase from *E. coli* showed that the cobalt(II) ions were bridged by a hydroxyl group (or a water molecule).

The same type of bridging between metal ions can be found in various hydrolytic Zn-enzymes that mediate the cleavage of amides, phosphates, antibiotics (β-lactams), and other biologically important substrates.[10–12] The μ-hydroxo (or μ-aquo) motif is the common feature of the metal cluster of the above-mentioned enzymes, for which distinct types of roles have been proposed. For instance, in the case of the zinc and cobalt hydrolases, it is often considered as the active nucleophile.[13] In the case of the copper enzymes, the hydroxyl group is labile and leaves the active site to allow substrate binding (dioxygen and catechol or tyrosine).[6,7]

Therefore, the synthesis and structural characterization of μ-hydroxo bridged dinuclear complexes is of special interest because they are useful as structural models of such metal clusters.[14] Furthermore, the magnetic characterization of these compounds is important to determine the type of magnetic interactions associated with such a bridge, information that is useful for understanding the physicochemical properties of the metalloproteins containing such metal dinuclear units.[15]

[a]*Departamento de Química Inorgánica, Facultade de Química, Universidade de Santiago de Compostela, 15782, Santiago de Compostela, España. E-mail: mrufina.bastida@usc.es*
[b]*Departamento de Química Inorgánica, Facultade de Química, Universidade de Vigo, 36310, Vigo, Pontevedra, España*
[c]*Departamento de Física, Facultad de Bioquímica y Ciencias Biológicas, Universidad Nacional del Litoral, Ciudad Universitaria, Paraje el Pozo, S3000ZAA Santa Fe, Argentina. E-mail: brondino@fbcb.unl.edu.ar*
[d]*REQUIMTE-CQFB, Departamento de Química, FCT-Universidade NOVA de Lisboa, 2829 Monte de Caparica, Portugal. E-mail: clodeiro@uvigo.es*
[e]*Grupo BIOSCOPE, Departamento de Química Física, Facultade de Ciencias, Universidade de Vigo, Campus de Ourense, E32004 Ourense, España*

† Electronic supplementary information (ESI) available: Additional data. CCDC reference numbers 780384 and 780385. For ESI and crystallographic data in CIF or other electronic format see DOI: 10.1039/c0dt00692k

As shown in Scheme 1, the macrocyclic $Py_2N_4S_2$, hereafter called L, is an octadentate ligand that has the capability to form dinuclear metal species, leaving enough room to accommodate a hydroxyl group in a bridging position between the two metal ions. As part of our ongoing project on the synthesis, characterization and studies of transition metal ion complexes oriented to mimic metal sites in metalloproteins,[16–18] and to learn about the structural, spectroscopic, and magnetic properties of μ-OH bridged dinuclear units, we report here the synthesis and the characterization of a novel family of Cu(II), Co(II) and Zn(II) complexes with ligand L, together with the respective mixed compounds.

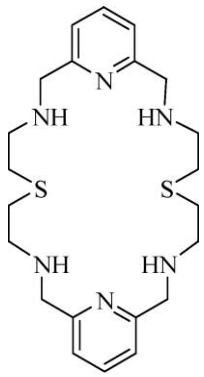

L

Scheme 1

Results and discussion

Synthesis and characterisation of the complexes

The coordination ability of ligand L towards hydrated tetrafluoroborate (M(II) = Co(II), Cu(II)) and nitrate (M(II) = Zn(II)) salts was studied. Reaction of L with M(II) tetrafluoroborates in a 2 : 1 metal-to-ligand ratio in nitromethane led to compounds with the formulas $[M_2L](BF_4)_4{\cdot}xH_2O$ ($[Co_2L](BF_4)_4{\cdot}8H_2O$ (**1**) and $[Cu_2L](BF_4)_4{\cdot}4H_2O$ (**2**)) in good yield (68 and 72%, respectively). Reaction of L with Zn(II) nitrate in a 2 : 1 metal-to-ligand ratio in ethanol led to the compound of formula $[Zn_2L](NO_3)_4.2C_2H_6O$ (**3**) in good yield (58%). Reaction of L with Cu(II) and Co(II) tetrafluoroborates and Zn(II) nitrate in a 1 : 1 : 1 metal-to-metal-to-ligand ratio in nitromethane led to compounds with the formulas $[CoZnL](BF_4)_2(NO_3)_2{\cdot}7H_2O$ (**4**), $[CuZnL](BF_4)_2(NO_3)_2{\cdot}6H_2O$ (**5**) and $[CoCuL](BF_4)_4{\cdot}2H_2O$ (**6**) in good yield (43–58%). The compounds were characterized by elemental analysis and IR, UV-Vis, ESI and MALDI-TOF spectra. The ESI and MALDI-TOF mass spectra display peaks that confirm the formation of all complexes. The IR spectra of all of the complexes show similar features. The presence of water molecules was confirmed by the appearance in the IR spectra of an intense broad band centred at *ca.* 3400 cm^{-1}. The bands due to the ν(C=N) and ν(C=C) stretching modes of the pyridine rings and to the ν(N–H) stretching modes of the amine groups are generally shifted to higher wavenumbers when compared to their position in the spectrum of the free ligand, suggesting coordination of these groups to the metal ions.[19] The IR spectra of the complexes show the presence of several bands in the region associated with tetrafluoroborate vibrations, either suggesting coordination to the metal ion or due to hydrogen bond interactions.[20] The spectra of the nitrate complexes show an intense band at 1380 cm^{-1}, with a shoulder at *ca* 1300 cm^{-1}, suggesting the presence of both coordinated and ionic nitrate groups.[21]

The molar conductance values for the complexes **1**, **2**, **4**, **5** and **6** measured in nitromethane and for the complex **3** measured in acetonitrile, at 25 °C, lie in the range reported as 2 : 1 electrolytes. This result suggests that two counterions are uncoordinated in solution.[22]

Crystals of $[Cu_2L(\mu\text{-}OH)(CH_3NO_2)_2](BF_4)_3{\cdot}H_2O$ (**7**) suitable for single-crystal X-ray diffraction were obtained by slow evaporation of a nitromethane solution of compound $[Cu_2L](BF_4)_4{\cdot}4H_2O$ (**2**).

The crystal structure of **7** contains the $[Cu_2L(\mu\text{-}OH))(CH_3NO_2)_2]^{3+}$ cation (Fig. 1) where two Cu(II) ions are located inside the macrocyclic cavity. Each Cu(II) ion is coordinated to one pyridine nitrogen atom, to two secondary amine nitrogen atoms and to one oxygen atom from a hydroxyl group acting as a bridge between the two metal centres. They are also weakly bonded to one sulfur atom and to one nitromethane molecule (with Cu–S distances of 2.7672(9) and 2.7259(8) Å and Cu–O distances of 2.931(2) and 2.807(2) Å). Taking into account all of these interactions, the coordination geometry is distorted

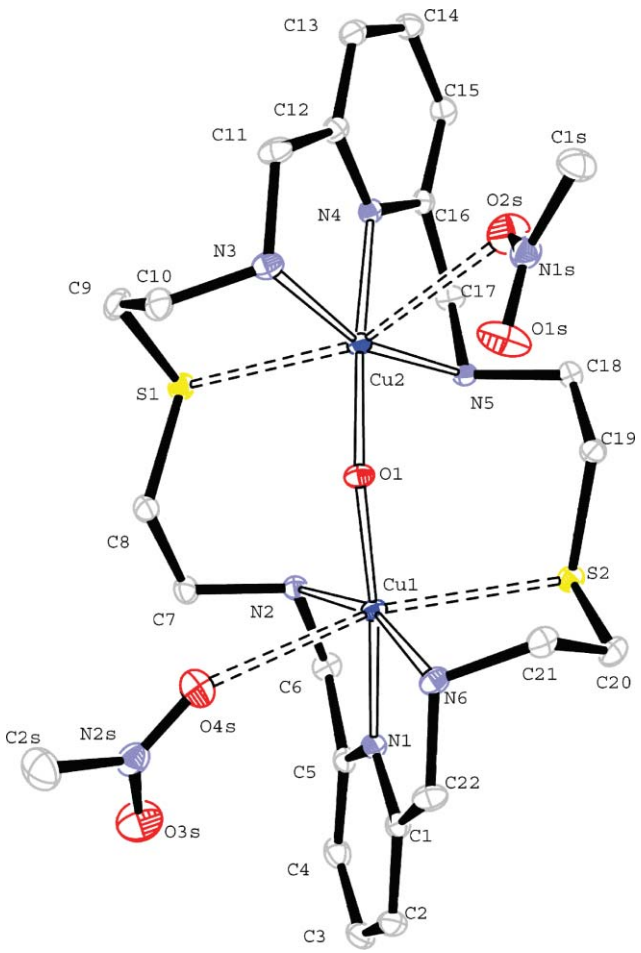

Fig. 1 Crystal structure of the $[Cu_2L(\mu\text{-}OH))(CH_3NO_2)_2]^{3+}$ cation. Ellipsoids are shown at the 50% probability level. Hydrogen atoms are omitted for clarity. Selected bond lengths and angles are given as ESI†.

octahedral. The dihedral angle between the planes containing the pyridine rings of the molecule is 50.88(5)° showing that the ligand is twisted. It is also folded, as the angle between the pyridine N atoms and the oxygen atom of the OH group acting as a bridge is 137.80(5)°.

Numerous hydrogen bonds are established between the oxygen atom of the free water molecule, the bridging hydroxyl group and the BF_4^- groups. The possible hydrogen bonds are given as ESI†. No π–π interactions are observed in the crystal lattice. Neighbouring dinuclear units are connected by chemical paths involving the above-mentioned H bonds.

Crystals of $[Zn_2L(\mu\text{-}OH)(H_2O)_2(NO_3)](NO_3)_2{\cdot}0.5H_2O$ (**8**) suitable for single-crystal X-ray diffraction were obtained by slow evaporation of a water solution of compound $[Zn_2L](NO_3)_4.2C_2H_6O$ (**3**).

Only one half of the dimer complex entity is present in the asymmetric unit. The molecular geometry is characterized by a crystallographic mirror plane running through the S atoms, the μ-OH hydroxo group and one nitrate anion, which generates by symmetry the second half of the complex moiety. The crystal structure of **8** contains the $[Zn_2L(\mu\text{-}OH)(H_2O)_2(NO_3)]^{2+}$ cation (Fig. 2) where two Zn(II) ions are sited into the macrocyclic cavity, coordinated to a pyridine nitrogen atom, to two secondary amine groups from the macrocyclic backbone, to one water molecule and to one hydroxide ion acting as a bridge between the two metal centres. They are also weakly bonded to one oxygen atom from the nitrate ion sited in a mirror plane, which then also acts as another bridge between the two symmetry-related metal centres (Zn–O1N, 2.647(8) Å). Considering this weak interaction, the geometry around the Zn(II) ions can then be considered as slightly distorted octahedral. The ligand is folded and the dihedral angle between the planes containing the pyridine rings of the molecule is 53.3(2)°. The dihedral angle between the planes containing the pyridine rings and the nitrate group located in the mirror plane between the two rings is 26.6(1)° (Fig. 2b). The distance between the centroid of one pyridine ring and the nitrogen atom of the nitrate group is 3.6 Å, suggesting the presence of π–π interactions between the electron clouds of the three groups. Intermolecular face-to-face π,π-stacking interactions have been found between the pyridine rings of adjacent molecules (Fig. 2b). The distance between the planes containing the aromatic rings is 3.40 Å, whilst the distance between centroids is 3.5 Å.

Also, hydrogen bond interactions have been observed between the oxygen atoms of the free nitrate ions and the secondary amine groups of the ligand and between the water molecule acting as a bridge between the two metal centres and the free water molecule. Possible hydrogen bonds are given as ESI†.

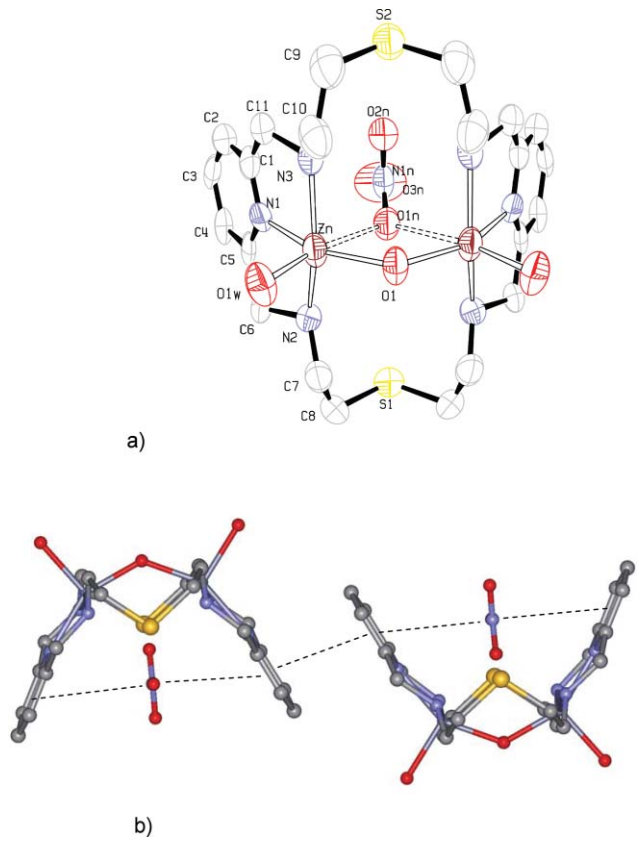

Fig. 2 (a) Crystal structure of the $[Zn_2L(\mu\text{-}OH)(H_2O)_2(NO_3)]^{2+}$ cation. Ellipsoids are shown at the 50% probability level. Hydrogen atoms are omitted for clarity. Selected bond lengths and angles are given as ESI†. (b) Crystal structure of $[Zn_2L(\mu\text{-}OH)(H_2O)_2(NO_3)](NO_3)_2{\cdot}0.5H_2O$ (**8**) showing the π,π-stacking interactions between the pyridine groups and the nitrate ions.

Spectrophotometric studies

The electronic spectra of the complexes **1** and **2** in ethanol were measured at room temperature (see ESI, Fig. S1†). In the UV region, the spectra show the band observed in the free ligand, centred at *ca* 260 nm (ε = 12058 M^{-1} cm^{-1}) and associated with the π–π* electronic transition of the pyridine rings present in the macrocyclic skeleton.[23] The spectrum of **1** exhibits one band at 344 nm (ε = 6451 M^{-1} cm^{-1}) assigned to a metal-to-ligand charge transfer band (MLCT) and another band at 478 nm (ε = 515 M^{-1} cm^{-1}) (see inset on Fig. S1†), assigned to one *d*–*d* transition band of the cobalt(II) ion. The position of the latter observed band suggests a coordination number of six for each metal centre.[24]

In the copper(II) complex **2**, in addition to the ligand band at 260 nm (ε = 13078 M^{-1} cm^{-1}), bands at 308 (ε = 2016 M^{-1} cm^{-1}) and 579 nm (ε = 210 M^{-1} cm^{-1}) were observed. The first band at 308 nm (ε = 2016 M^{-1} cm^{-1}) is assigned to a metal-to-ligand charge transfer band (MLCT) while the broad band observed at 579 nm (ε = 210 M^{-1} cm^{-1}) was assigned to the $^2T_{2g} \leftarrow {}^2E_g$ *d*–*d* transition band of the copper(II) ions. This suggests a coordination number of six in solution for the metal centres, however, due to the Jahn–Teller effect present in the Cu(II) complexes, this band could also be indicative of a tetragonal distortion for each copper centre.[24]

Metal titrations monitored by UV-vis spectroscopy were performed in order to explore the coordination properties of ligand L (Fig. 3 and Fig. 4). The absorbance variation at 267 and 344 nm for the Co(II) complex and at 261 and 308 nm for the Cu(II) complex as a function of the number of metal equivalents added to the solution is consistent with the formation of 1 : 2 L : M complexes (see insets on Fig. 3 and Fig. 4).

MALDI-TOF-MS studies

As a general rule, a MALDI-TOF matrix is a small organic compound that absorbs the energy in the UV region (337 nm N_2

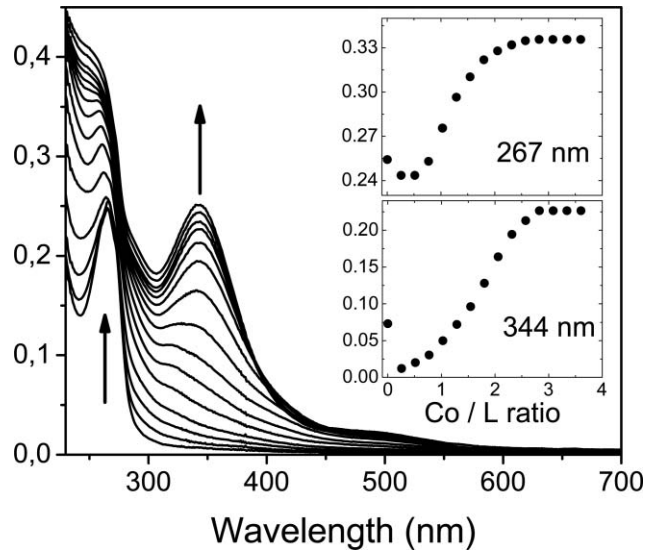

Fig. 3 Absorption spectra of an ethanolic solution of L as a function of increasing amounts of $Co(BF_4)_2{\cdot}6H_2O$. The insets show the absorbance at 267 and at 344 nm. The arrows show the changes experienced by the absorption bands at increasing metal amounts. ([L] = $5.00{\cdot}10^{-5}$ M, T = 298 K).

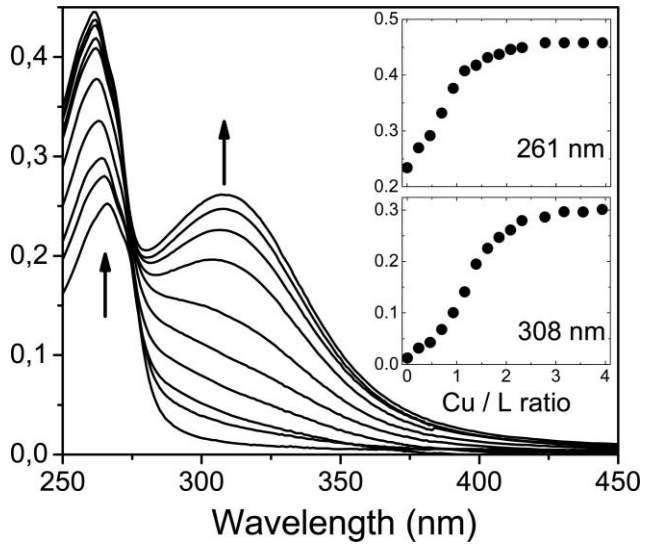

Fig. 4 Absorption spectra of an ethanolic solution of L as a function of increasing amounts of $Cu(BF_4)_2{\cdot}6H_2O$. The insets show the absorbance at 261 and at 308 nm. The arrows show the changes experienced by the absorption bands at increasing metal amounts. ([L] = $4.32{\cdot}10^{-5}$ M, T = 298 K).

laser). An advance in the study by MALDI-TOF-MS spectrometry of supramolecular complexes with organic ligands provided with UV chromophores is that the ligand acts at the same time as the ligand and MALDI matrix.[25] For the compounds studied here we used dithranol as the MALDI matrix, because the energy absorption of the two pyridine rings of the macrocyclic ligand is not strong enough to act as a matrix. Metal ion titrations monitored by MALDI-TOF mass spectrometry were performed using aqueous solutions of ligand L. The samples were dissolved in ethanol (1–2 mg mL^{-1}) and dithranol was added to obtain the

Table 1 Crystal data and structure refinement for $[Cu_2L(\mu\text{-}OH)(CH_3NO_2)_2](BF_4)_3{\cdot}H_2O$ (**7**) and $[Zn_2L(\mu\text{-}OH)(H_2O)_2(NO_3)](NO_3)_2{\cdot}0.5H_2O$ (**8**)

	7		**8**
Empirical formula	$C_{24}\ H_{43}\ B_3\ N_8\ O_6\ Cu_2\ F_{12}\ S_2$		$C_{22}\ H_{40}\ N_9\ O_{12.5}\ Zn_2\ S_2$
Formula weight	991.29		825.49
Temperature/K	100(2)		100(2)
Wavelength/Å	0.71073		0.71073
Crystal system	Triclinic		Orthorhombic
Space group	$P\bar{1}$		Pnma
Unit cell dimensions	a = 10.711(5) Å	α = 67.947(5)°	a = 17.056(10) Å
	b = 12.273(5) Å	β = 86.665(5)°	b = 21.052(8) Å
	c = 16.182(5) Å	γ = 70.868(5)°	c = 9.149(5) Å
Volume/Å^3	1857.6(13)		3284.9
Z	2		4
Density (calculated)/g cm^{-3}	1.772		1.669
Absorption coefficient/mm^{-1}	1.369		1.662
F(000)	1008		1708
Crystal size/mm^3	0.56 × 0.49 × 0.09		0.17 × 0.07 × 0.03
Theta range for data collection/°	1.36–28.28		1.93–21.03
Index ranges	$-14 \le h \le 14$.		$-13 \le h \le 17$,
	$-14 \le k \le 16$.		$-21 \le k \le 21$,
	$0 \le l \le 21$		$-9 \le l \le 8$
Reflections collected	40 182		11 632
Independent reflections	9162 [R_{int} = 0,0271]		1833 [R_{int} = 0.0994]
Completeness (to theta)	99.3% (28.28°)		100.0% (21.03°)
Absorption correction	Empirical (Sadabs)		Empirical (Sadabs)
Max. and min. transmission	0.8867 and 0.5144		0.9518 and 0.7654
Refinement method	Full-matrix least-squares on F^2		Full-matrix least-squares on F^2
Data/restraints/parameters	9162/0/574		1833/0/240
Goodness-of-fit on F^2	1.070		1.001
Final R indices [$I > 2\sigma(I)$]	R_1 = 0.0259, wR_2 = 0.0641		R_1 = 0.0524, wR_2 = 0.1289
R indices (all data)	R_1 = 0.0319, wR_2 = 0.0661		R_1 = 0.1106, wR_2 = 0.1608
Largest diff. peak and hole/eÅ^{-3}	0.484/–0.692		0.582/–0.365

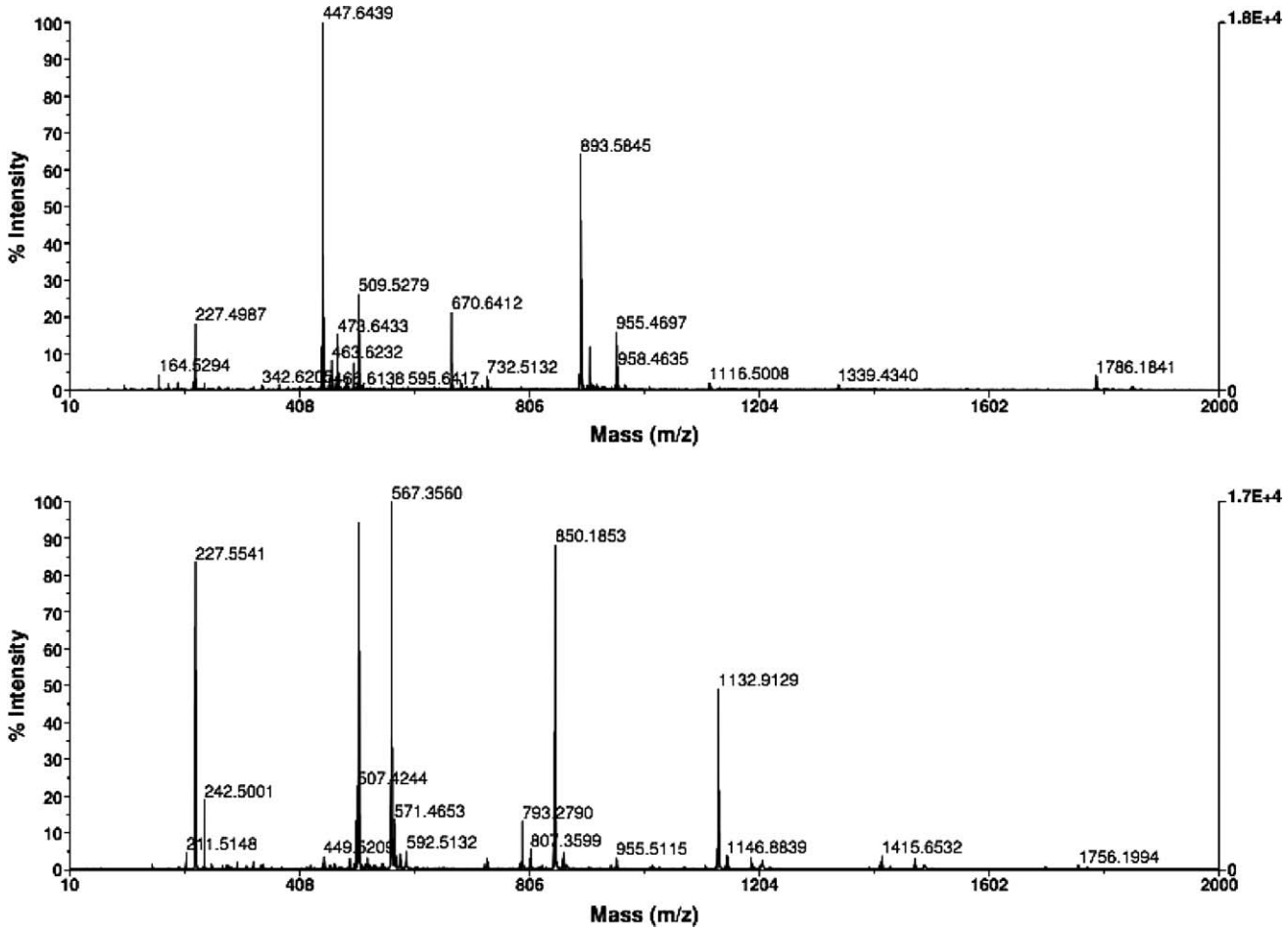

Fig. 5 MALDI-TOF-MS spectra of L using dithranol as MALDI matrix (top) and in the presence of one equivalent of Co(II) and one equivalent of Cu(II) (bottom).

mass spectra. A solid layer of the ligand + matrix was deposited on the MALDI-TOF-MS plate after drying off the water, followed by superposition of a second solid layer of the aforementioned metal ions dissolved in water. Molar ratios (L : M) of 1 : 1 and 1 : 2 were used. An *in situ* MALDI-TOF reaction on the system takes place upon laser irradiation and formation of the metal complexes was observed with ligand L. Fig. 5 shows the MALDI spectra for the ligand L and for the Cu(II) and Co(II) compounds with L in a 1 : 1 : 1 ratio. All of the peaks observed by MALDI-TOF-MS metal titrations are shown in Table 2. As seen in this table, the peaks attributed to the species $[ML]^+$ and $[M_2L]^+$ were observed for all of the complexes, indicating that they are stable in these conditions. These results also indicate that the complex formation is sequential, *i.e.* the monomer species is firstly formed, with the subsequent dimer formation upon addition of the second metal equivalent.

Table 2 Major peaks observed in the metal (M) titration of L obtained by MALDI-TOF-MS using dithranol as the matrix[a]

Metal titration	L (a.m.u.)		L+M (a.m.u.)		L+2M (a.m.u.)	
Co(II)	$[LH]^+$	447.64	$[CoL]^+$	504.59	$[Co_2L]^+$	564.40
Cu(II)	$[LH]^+$	447.64	$[CuL]^+$	509.60	$[Cu_2L]^+$	576.46
Zn(II)	$[LH]^+$	447.64	$[ZnL]^+$	509.56	$[Zn_2L]^+$	577.51
Co(II)/Cu(II)	$[LH]^+$	447.64	$[CoL]^+$	504.59	$[CoCuL]^+$	567.35
Co(II)/Zn(II)	$[LH]^+$	447.64	$[CoL]^+$	504.59	$[CoZnL]^+$	572.42
Cu(II)/Zn(II)	$[LH]^+$	447.64	$[CuL]^+$	509.60	$[CuZnL]^+$	577.22

[a] X_1 = matrix = 1,8,9-Trihydroxyanthracene (Dithranol) = $C_{14}O_3H_{10}$

Magnetic properties

$[Co_2L](BF_4)_4 \cdot 8H_2O$ (1). Fig. 6 shows the inverse of the magnetic susceptibility χ of **1** and the product χT, both as a function of temperature. As seen in the χT *vs.* T plot, χT decreases on cooling; the lower the temperature, the more pronounced this effect. The magnetic susceptibility data of **1** could be well accounted for using the Curie–Weiss law, $\chi(T) = C/(T\text{-}\theta)$, where C is the Curie constant and θ is the Weiss temperature.[38] Least squares fitting of this expression to the experimental data of $\chi^{-1}(T)$ *vs* T, yielded the parameters $C = 10.00 \pm 0.03$ emu K mol^{-1} and $\theta = -11.8 \pm 0.6$ K. The negative value of θ suggests antiferromagnetic interactions between the Co(II) ions, as seen in the χT *vs.* T plot, although zero field splitting can also cause similar effects.

From the Curie constant value, we obtained $g = 4.62 \pm 0.01$, which is typical for Co(II) ions in high spin configuration ($S = 3/2$). The magnetic data can also be interpreted assuming a dinuclear model of $S_1 = S_2 = 3/2$, as suggested by the chemical

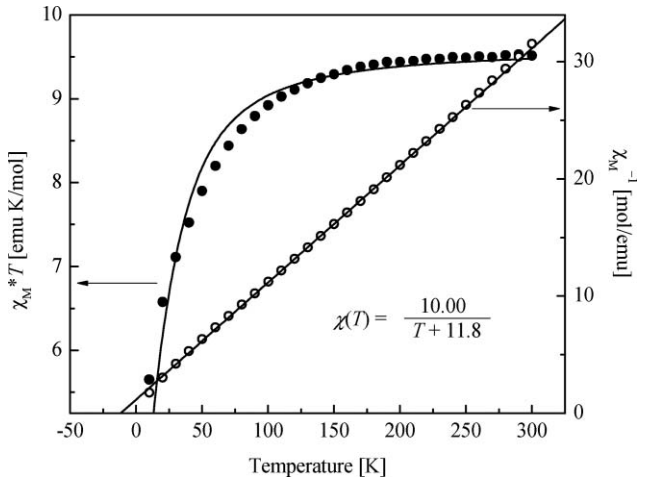

Fig. 6 Temperature dependence of the χT (solid circles) and χ^{-1} (open circles) for $[Co_2L](BF_4)_4{\cdot}8H_2O$ (**1**). The solid lines were obtained by least squares fitting as explained in the text.

characterization of this compound, using a spin Hamiltonian with axial zero field splitting

$$H = \sum_{i=1}^{2}\left\{D_i\left[S_{iz}^2 - \frac{S_i(S_i+1)}{3}\right] + g_i\mu_B \vec{S}_i.\vec{H}\right\} - J\vec{S}_1.\vec{S}_2 \qquad (1)$$

where all the symbols have their usual meaning.[26] Assuming $D_1 = D_2$ and $g_1 = g_2$, the parameters were optimized to fit the χT *vs.* T curve (see Fig. 7). This procedure gave $g = 3.21$, $J = -0.97$ cm^{-1} and $D = 31.2$ cm^{-1}. This result indicates weak antiferromagnetic interactions between the Co(II) ions, as suggested by the Curie–Weiss analysis. There is not as much work published on the magneto-structural correlations in dinuclear cobalt(II) complexes as is the case for Cu(II) dimer complexes. The value for the coupling constant J obtained here is in line with those found in the literature for cobalt(II) dimers[26,27] and gives an additional support for the dimeric nature of **1**.

Fig. 7a shows the EPR spectrum obtained at 10 K in a powder sample of **1**. No EPR signal is observed above 60 K. The powder spectrum shows two features. The more intense signal centred at ~1500 G corresponds to Co(II) ions in high spin configuration ($S = 3/2$). This signal is nearly axial with $g_\perp \sim 4.8 \cdot g_{//}$ and cannot be precisely determined because it is overlapping the second signal. This high spin component corresponds to a $\pm 1/2$ ground state with axial ZFS ($D > 0$, $E \sim 0$) in line with susceptibility data. A second signal with lower intensity is detected in the region 2200–3500 G. The g-values corresponding to this signal resemble those signals obtained for Co(II) ions in low spin configuration.[28] Partially solved hyperfine structure is observed between 2000 and 3500 G suggesting that the $g_{//}$ feature of the high spin component and the putative low spin signal may have overlapped their hyperfine structure, which precludes a precise determination of the parameters. The EPR data show that only a small fraction of the molecules adopt the low spin configuration and hence its contribution to the susceptibility data can be neglected.

$[Cu_2L(\mu\text{-}OH)(CH_3NO_2)_2](BF_4)_3{\cdot}H_2O$ (7). The magnetic data of **7** were analyzed taking into account a dominant isotropic interaction J in the assembly of a dinuclear unit ($S_1 = S_2 = \frac{1}{2}$)

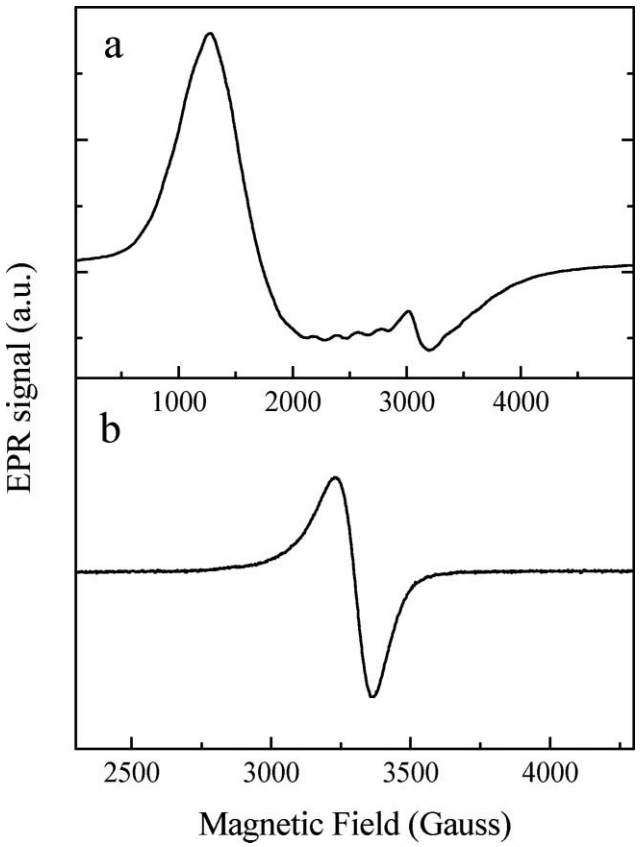

Fig. 7 EPR spectra of powder samples of (a) $[Co_2L](BF_4)_4{\cdot}4H_2O$ (**1**) and (b) $[Cu_2L(\mu\text{-}OH)(CH_3NO_2)_2](BF_4)_3{\cdot}H_2O$ (**7**).

with weak interdimer interactions characterized by the coupling constant J'. The spin Hamiltonian takes the form:

$$H = -J\vec{S}_1.\vec{S}_2 + g\mu_B\vec{S}.\vec{H} - zJ'\langle S_z\rangle\vec{S}_z \qquad (2)$$

All the symbols in eqn (2) have their usual meaning. The third term describes the intermolecular interactions in the molecular field approximation where z is the number of the nearest neighbours around a given dimer of the crystal cell.[38] The magnetic susceptibility $\chi(T)$ of **7** was calculated through the expression

$$\chi(T) = 2Ng^2\mu_B^2[kT - \frac{2zJ'}{3+\exp(-J/kT)}]^{-1}[3+\exp(-J/kT)]^{-1} \qquad (3)$$

where all the symbols have the usual meaning.[38] Least squares fitting of eqn (3) to the χT data (Fig. 8) gave the parameters $g = 2.179 \pm 0.003$, $J = 41 \pm 1$ cm^{-1}, and $J' = -0.12 \pm 0.01$ cm^{-1}. As shown in the inset on Fig. 8, χT increases on cooling as expected for ferromagnetic behaviour, reaching a maximum at $T \sim 10$ K. From this temperature and below, the magnetic susceptibility begins to decrease. The maximum in the χT *vs.* T curve at low temperatures characterizes a weak antiferromagnetic intermolecular interaction in a ferromagnetically coupled dimer and is observed instead of the plateau expected in the temperature range where only the triplet state $S = 1$ is thermally populated.

Fig. 7b shows the EPR spectrum obtained for a powder sample of **7** at 293 K. Similar spectra were observed in the temperature range of 4–293 K (not shown). The temperature variation of the

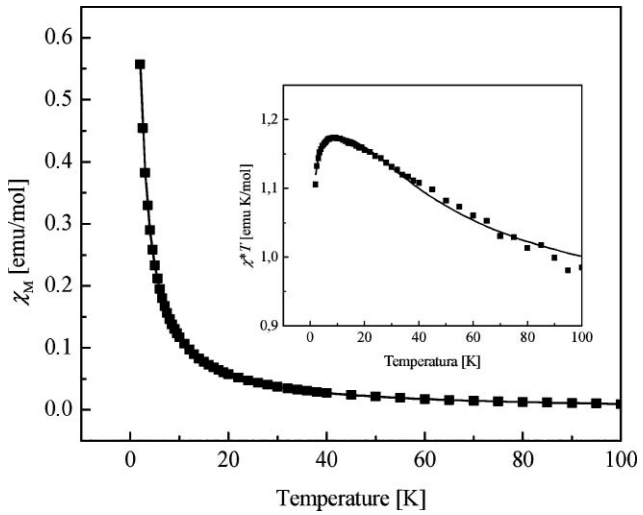

Fig. 8 Temperature dependence of χ and the product χT (inset) for $[Cu_2L(\mu\text{-}OH)(CH_3NO_2)_2](BF_4)_3\cdot H_2O$ (**7**). The solid lines were obtained by least squares fitting as explained in the text.

EPR line intensity (obtained as the second integral) multiplied by the temperature reproduces the data shown in the inset on Fig. 8 well, in line with the magnetic susceptibility data. As seen in Fig. 7b the powder spectrum shows a nearly isotropic signal at g = 2.090. This spectrum does not show the typical fine structure of a dimer system, determined by dipolar and anisotropic and antisymmetric interactions.[29] The two latter contributions can be neglected for dinuclear copper systems with an intradimer exchange interaction of $J \leq 30$ cm^{-1}, or thereabouts.[30] Therefore, the maximal value expected for the zero field splitting assuming the point dipole approximation with a Cu(II)–Cu(II) distance of 3.509 Å in **7** is estimated to be ~0.1 cm^{-1}, in the order of the interdimeric exchange interaction ($J' = -0.12$ cm^{-1}). This indicates that J' is strong enough to collapse the fine structure on the EPR spectra, as well as the hyperfine structure expected for the copper nuclei ($I = 3/2$), and explain the lack of solved fine and hyperfine structure in the EPR spectrum. This J' value is associated with weak exchange interactions, transmitted by the chemical paths connecting the neighbouring dinuclear units (see the structural description of the compound).

Many experimental and theoretical works performed on dihydroxo-bridged dicopper(II) complexes have shown that the value of the angle Cu–O–Cu in the Cu_2O_2 core and the out-of-plane deviation of the hydrogen atom of the OH moiety determine the nature, ferro- or antiferromagnetic, of the intradimer magnetic coupling.[31] Fewer examples exist regarding the magnetic properties of single hydroxo-bridged dicopper(II) compounds, but a similar trend to that of Cu_2O_2 cores has been observed.[32] The ferromagnetic behaviour found experimentally in **7** was unexpected and constitutes a rare example of a ferromagnetically coupled copper dinuclear complex with such bridging topology (Cu–O–Cu angle ~ 135°). A similar conclusion was obtained from the DFT calculations that we performed to evaluate the magnetic coupling constant of **7**. The calculations showed that the situation where the H atom of the μ-OH bridge is nearly included in the Cu–O–Cu plane and is stabilized by hydrogen bonding with the free water molecule is energetically favourable, with satisfactory spin contamination, distribution values and stable wavefunctions. In this situation, H in plane, $J = -280$ cm^{-1} was obtained, in contrast with the ferromagnetic behaviour found experimentally for **7**.

Similar unexpected results were found by Chaudhuri *et al.* for the dinuclear Cu(II) tautomers presenting di-μ-hydroxo and μ-aqua-μ-oxo bridges.[33] These authors proposed that the antiferromagnetic coupling observed for the tautomer with the $(\mu\text{-}OH)_2$ bridge is turned into ferromagnetic coupling in the tautomer with the $(\mu\text{-}OH_2)(\mu\text{-}O)$ bridge, which implies that the transfer of one proton from one of the two hydroxo bridges to the other gives rise to an asymmetric structure with totally different magnetic properties. These experimental results were more recently theoretically analyzed and critiqued by Rodríguez–Fortea *et al.*,[34] who suggest that the tautomer with the $(\mu\text{-}OH_2)(\mu\text{-}O)$ bridge is energetically unfavourable and that the unexpected magnetic behaviour could be produced by packing forces in the crystal lattice that distort the $(\mu\text{-}OH)_2$ bridge, leading to a ferromagnetic interaction. We cannot discard that this could also be occurring in the Cu(II) dinuclear compound studied here, since a free water molecule is within a hydrogen bond distance with the bridging hydroxo group and is also interacting *via* H bonds with the BF_4^- groups. This interaction could pull the H atom out of the Cu–O–Cu plane, a fact that has been reported as an important feature to be taken into account, especially in determining the ferro- or antiferromagnetic behaviour of μ-hydroxo bridged Cu(II) dinuclear compounds.[31c]

Conclusions

New dinuclear Cu(II), Co(II) and Zn(II) complexes with the $Py_2N_4S_2$ macrocyclic ligand, together with the respective mixed compounds, have been synthesized and characterized. The physicochemical characterization of these compounds suggests dinuclear units with a single μ-hydroxo motif in a bridging position between the two metal ions, as observed in several dinuclear metal clusters of copper, cobalt, and zinc metalloenzymes. In this case, this behaviour was only proved for compounds **7** and **8**.

The crystal structures of $[Cu_2L(\mu\text{-}OH)(CH_3NO_2)_2](BF_4)_3\cdot H_2O$ (**7**) and $[Zn_2L(\mu\text{-}OH)(H_2O)_2(NO_3)](NO_3)_2\cdot 0.5H_2O$ (**8**) were solved by single-crystal X-ray diffraction and show the metal ions in slightly distorted square planar and square pyramidal geometries, respectively.

Taking into account the results obtained by MALDI-TOF-MS spectrometry, ligand L can be explored as a chelating unit for cobalt(II), copper(II) and zinc(II) in the gas phase.

The magnetic characterization of the Co(II) compound points to a weakly antiferromagnetic dinuclear structure, with a coupling constant similar to those measured for other Co(II) dimer compounds. The magnetic data of the dinuclear Cu(II) compound revealed a ferromagnetically coupled dimer with weak antiferromagnetic intermolecular interactions. The intra-dimer ferromagnetic behaviour ($J = 41$ cm^{-1}) found for this Cu(II) dinuclear system was unexpected for a compound with such bridging topology. Our results suggest that the unexpected behaviour could be originating from non covalent interactions between the bridging moiety, lattice free water molecules and counterions and the packing forces that determine the sign and magnitude of the intradimeric exchange interaction.

Experimental

Measurements

Elemental analyses were performed on a Fisons Instruments EA1108 microanalyser by the Universidade de Santiago de Compostela. IR spectra were recorded as KBr discs on a BIO-RAD FTS 175-C spectrometer. FAB mass spectra were recorded using a KRATOS MS50TC spectrometer with 3-nitrobenzyl alcohol as the matrix. Conductivity measurements were carried out in 10^{-3} mol dm^{-3} nitromethane and acetonitrile solutions at 20 °C using a WTW LF3 conductivimeter. MALDI-TOF-MS spectra have been performed in a MALDI model Voyager DE-PRO Biospectrometry Workstation equipped with a nitrogen laser radiating at 337 nm from Applied Biosystems (Foster City, United States) by the MALDI-TOF-MS Service of the REQUIMTE, Chemistry Department, Universidade Nova de Lisboa. The acceleration voltage was 2.0×10^4 kV with a delayed extraction (DE) time of 200 ns. The spectra represent accumulations of 5×100 laser shots. The reflection mode was used. The ion source and flight tube pressures were less than 1.80×10^{-7} and 5.60×10^{-8} Torr, respectively. The MALDI mass spectra of the soluble samples (1 or 2 mg mL^{-1}) such as the ligand and metal complexes were recorded using the conventional sample preparation method for MALDI-MS. For the metal titrations by MALDI, 1 mL of the metal sample were put on the sample holder on which the chelating ligand had been previously spotted with the matrix 1,8,9-trihydroxyanthracene (dithranol). The sample holder was inserted in the ion source. Chemical reaction between the ligand and metal salts occurred in the holder and complex species were produced. Absorption spectra were recorded either on a Shimadzu UV-2501PC or on a Perkin Elmer lambda 35 spectrophotometer. All measurements were performed at 298 K.

Chemicals and starting materials

Macrocycle L was synthesized as previously reported.[35] 2,6-pyridinedimethanol, 1,5-diamine-3-thiopentane and hydrated tetrafluoroborate salts were commercial products (ABCR or Aldrich). Solvents used were of reagent grade and purified by the usual methods.

Synthesis

Synthesis of the tetrafluoroborate metal complexes of L. General procedure

The tetrafluoroborate metal salt (0.08 mmol) was dissolved in nitromethane (5 mL) and added to a stirred solution of the ligand L (0.04 mmol) in nitromethane (25 mL). The solution was softly heated and stirred for 4 h. The solution was concentrated in a rotary evaporator until the volume was *ca* 5 mL. Diethyl ether was added to the solution and the resulting solid product obtained was isolated by centrifugation and dried under vacuum.

[Co_2L](BF$_4$)$_4$·8H$_2$O (1). Yield: 68% (Found: C 24.3, H 4.8, N 8.4, S 5.9. Calc. for $C_{22}H_{50}N_6O_8S_2B_4F_{16}Co_2$: C 25.0, H 4.8, N 8.0, S 6.0%); Conductivity (CH_3NO_2, 1.10^{-3} M): 156 μS cm^{-1} (2 : 1); ν_{max}/cm^{-1} 1608, 1458 [ν(C═N)$_{py}$ and ν(C═C)], 2929, 2860 [ν(NH)], 1122, 1083, 1063, 1040, 785 [ν(BF$_4^-$)]; UV-vis (H_2O) λ = 251 nm (ε = 13 068 M^{-1} cm^{-1}), λ = 257 nm (ε = 13 257 M^{-1} cm^{-1}), λ = 263 nm (ε = 12 197 M^{-1} cm^{-1}), λ = 321 nm (ε = 6020 M^{-1} cm^{-1}), λ = 478 nm (ε = 548 M^{-1} cm^{-1}); *m*/*z* (ESI) 447 [L+H]$^+$, 504 [CoL]$^+$, 591 [CoL(BF$_4$)]$^+$, 646 [Co_2L(BF$_4$)]$^+$, 730 [Co_2L(BF$_4$)$_2$]$^+$; *m*/*z* (MALDI) (dithranol): 504 [CoL]$^+$, 567 [Co_2L]$^+$, 793 [Co_2L(dithranol)]$^+$, 870 [Co_2L(BF$_4$)(dithranol)]$^+$, 1133 [Co_2L(BF$_4$)$_4$(dithranol)]$^+$. Colour: red.

[Cu_2L](BF$_4$)$_4$·4H$_2$O (2). Yield: 72% (Found: C 26.6, H, 4.3, N 8.3, S 6.3. Calc. for $C_{22}H_{42}N_6O_4S_2B_4F_{16}Cu_2$: C 26.6, H 4.3, N 8.4, S 6.4%). Conductivity (CH_3NO_2, 10^{-3} M): 178 μS cm^{-1} (2 : 1); ν_{max}/cm^{-1}: 1606, 1473 [ν(C═N)$_{py}$ and ν(C═C)], 2921, 2865 [ν(NH)], 1123, 1083, 1038, 801 [ν(BF$_4^-$)]; UV-vis (H_2O) λ = 257 nm (ε = 12929 M^{-1} cm^{-1}); λ = 327 nm (ε = 2140 M^{-1} cm^{-1}); λ = 620 nm (ε = 179 M^{-1} cm^{-1}); *m*/*z* (ESI) 447 [L+H]$^+$, 509 [CuL]$^+$, 596 [CuL(BF$_4$)]$^+$, 657 [CuL(BF$_4$)(CH$_3$NO$_2$)]$^+$, 763 [Cu_2L(BF$_4$)$_2$(OH)]$^+$; *m*/*z* (MALDI) (dithranol): 509 [CuL]$^+$, 573 [Cu_2L]$^+$. Colour: blue–green.

Synthesis of the nitrate Zn(II) complex of L. General procedure

The nitrate Zn(II) salt (0.08 mmol) was dissolved in ethanol (5 mL) and added to a stirred solution of the ligand L (0.04 mmol) in ethanol (25 mL). In this case the appearance of one precipitate was observed immediately after the addition of the metal salt. The solution was softly heated and stirred for 4 h. The white precipitate formed was isolated by filtration yielding the metal complexes of the ligand.

[Zn_2L](NO$_3$)$_4$.2C$_2$H$_6$O (3). Yield: 58% (Found: C 34.1, H 4.8, N 15.6, S 8.2. Calc. for $C_{26}H_{46}N_{10}O_{14}S_2Zn_2$: C 34.1, H 5.0, N 15.3, S 7.0%); Conductivity (CH_3CN, 10^{-3} M): 292 μS cm^{-1} (2 : 1); ν_{max}/cm^{-1}: 1607, 1467 [ν(C═N)$_{py}$ and ν(C═C)], 2917, 2833 [ν(NH)], 1300, 1384 [ν(NO$_3^-$)]; *m*/*z* (MALDI) 447 [L+H]$^+$, 509 [ZnL]$^+$, Colour: white.

Synthesis of the mixed metal complexes of the type [(M$_1$M$_2$)L](BF$_4$)$_n$(NO$_3$)$_{n'}$·xH$_2$O. General procedure

The appropriate metal salts M_1 and M_2 (0.04 mmol, 0.04 mmol) were dissolved in nitromethane (10 mL) and added to a stirred solution of the ligand L (0.04 mmol) in nitromethane (25 mL). The resulting solution was concentrated in a rotary evaporator until the volume was *ca.* 5 mL. Diethyl ether was added to the solution and the resulting solid product obtained was isolated by centrifugation and dried under vacuum.

[CoZnL](BF$_4$)$_2$(NO$_3$)$_2$·7H$_2$O (4). Yield: 58% (Found: C 26.6, H 4.3, N 11.9, S 5.1. Calc. for $C_{22}H_{48}N_8O_{13}S_2B_2F_8CoZn$: C 26.6, H 4.8, N 11.3, S 6.4%); Conductivity (CH_3NO_2, 10^{-3} M): 175 μS cm^{-1} (2 : 1); ν_{max}/cm^{-1} 1609, 1479 [ν(C═N)$_{py}$ and ν(C═C)], 2915, 2838 [ν(NH)], 1038, 1061, 1083 [ν(BF$_4^-$)], 1384 [ν(NO$_3^-$)]; UV-vis (H_2O) λ = 258 nm (ε = 17817 M^{-1} cm^{-1}); λ = 322 nm (ε = 8294 M^{-1} cm^{-1}); λ = 471 nm (ε = 753 M^{-1} cm^{-1}); *m*/*z* (ESI): 447 [L]$^+$, 503 [CoL]$^+$, 571 [CoZnL]$^+$, 865 [CoZnL(BF$_4$)$_2$(NO$_3^-$)$_2$]$^+$; *m*/*z* (MALDI) (dithranol): 504 [CoL]$^+$, 807 [CoZnL(BF$_4$)$_2$(NO$_3^-$)]$^+$. Colour: brown.

[CuZnL](BF$_4$)$_2$(NO$_3$)$_2$·6H$_2$O (5). Yield: 43% (Found: C 26.6, H 4.8, N 12.3, S 6.6. Calc. for $C_{22}H_{46}N_8O_{12}S_2B_2F_8CuZn$: C 26.9, H 4.7, N 11.4, S 6.5%); Conductivity (CH_3NO_2, 10^{-3} M): 183 μS cm^{-1} (2 : 1); ν_{max}/cm^{-1} 1608, 1475 [ν(C═N)$_{py}$ and ν(C═C)], 2922, 2845 [ν(NH)], 1037, 1060 [ν(BF$_4^-$)], 1388 [ν(NO$_3^-$)];

UV-vis (H_2O) λ = 261 nm ($\varepsilon \approx 9322$ M^{-1} cm^{-1}); λ = 326 nm ($\varepsilon \approx 1448$ M^{-1} cm^{-1}); λ = 612 nm ($\varepsilon \approx 112$ M^{-1} cm^{-1}); *m/z* (ESI): 446 $[L]^+$, 508 $[CuL]^+$, 596 $[CuL(BF_4)]^+$, 765 $[CuZnL(BF_4)_2(OH)]^+$; *m/z* (MALDI) (dithranol): 468 $[NaL]^+$, 509 $[CuL]^+$, 571 $[Cu_2L]^+$, 895 $[NaCuZnL(BF_4)_2(NO_3^-)_2]^+$. Colour: blue.

$[CoCuL](BF_4)_4 \cdot 2H_2O$ (6). Yield: 52% (Found: C 27.4, H 4.5, N 9.4, S 5.9. Calc. for $C_{22}H_{38}N_6O_2S_2B_4F_{16}CoCu$: C 27.7, H 4.0, N 8.8, S 6.7%); Conductivity (CH_3NO_2, 10^{-3} M): 101 μS cm^{-1}; ν_{max}/cm^{-1} 1608, 1473 [ν(C=N)$_{py}$ and ν(C=C)], 2928, 2852 [ν(NH)], 1123, 1081, 1039, 801 [$\nu(BF_4^-)$]; UV-vis (H_2O) λ = 255 nm (ε = 17028 M^{-1} cm^{-1}); λ = 318 nm (ε = 5577 M^{-1} cm^{-1}); λ = 475 nm (ε = 307 M^{-1} cm^{-1}); λ = 633 nm (ε = 154 M^{-1} cm^{-1}); *m/z* (ESI): 467 $[NaL]^+$, 529 $[NaCoL]^+$, 571 $[CoCuL]^+$; *m/z* (MALDI) (dithranol): 449 $[L]^+$, 510 $[CuL]^+$, 567 $[CoCuL]^+$, 793 [CoCuL(dithranol)]$^+$, 850 $[NaCoCuL(BF_4)_3]^+$. Colour: blue.

Crystal structure determinations of $[Cu_2L(\mu\text{-}OH)(CH_3NO_2)_2](BF_4)_3 \cdot H_2O$ (7) and $[Zn_2L(\mu\text{-}OH)(H_2O)_2(NO_3)](NO_3)_2 \cdot 0.5H_2O$ (8)

Crystals of $[Cu_2L(\mu\text{-}OH)(CH_3NO_2)_2](BF_4)_3 \cdot H_2O$ (**7**) and $[Zn_2L(\mu\text{-}OH)(H_2O)_2(NO_3)](NO_3)_2 \cdot 0.5H_2O$ (**8**) suitable for single-crystal X-ray diffraction were obtained by slow evaporation of a nitromethane solution of **2** and a water solution of **3**, respectively. Measurements were performed on a Bruker SMART CCD 1000 area diffractometer. single-crystal X-ray crystal data details, structure solution and refinement for **7** and **8** are given in Table 1. All data were corrected for Lorentz and polarization effects. Empirical absorption corrections were also applied for both crystal structures.[36] Complex scattering factors were taken from the program package SHELXTL.[37] The structures were solved by direct methods, which revealed the position of all non-hydrogen atoms. All the structures were refined on F^2 by a full-matrix least-squares procedure using anisotropic displacement parameters for all non-hydrogen atoms. The hydrogen atoms attached to the carbon atoms were located in their calculated positions and refined using a riding model whereas the hydrogen atoms attached to the oxygen and nitrogen atoms were localized in a Fourier map and refined independently. One of the three tetrafluoroborate anions present in the asymmetric unit was modelled as disordered in two positions.

Magnetic and EPR Measurements

Temperature-dependent magnetic susceptibilities of powder samples were measured using a PPMS (Quantum Design Physical Property Measurement System) susceptometer in the range 10–300 K under an applied field of 500 mT for the cobalt compound and in the range 2–300 K under an applied field of 300 mT for the copper compound. Pascal's constants were used to estimate the correction of the underlying diamagnetism of the compounds.[38]

EPR measurements at 9.65 GHz of powder samples were performed on a Bruker EMX spectrometer using a rectangular cavity with 100 kHz field modulation and equipped with an Oxford continuous helium flow cryostat. Temperatures were 4 K for the cobalt compound and 293 K and 77 K for the copper compound. The solid samples used in the magnetic and EPR measurements for the copper compound were obtained by grinding single crystals of **7**.

DFT calculations

DFT calculations were performed using the hybrid B3LYP functional[39] and 6-31G** basis set as implemented in Gaussian 03 package.[40] With the exception of the structure optimizations, all energy calculations were performed with tight convergence criteria owing to the small magnitude of the coupling constant obtained by consideration of the magnetic susceptibility. For the calculations, the atom coordinates from the crystallographic data were used as a model, and all of the atoms were included in the structure optimization, with the exception of the disordered BF_4^- molecule. Only the positions of the hydrogen atoms of the oxygenic μ-OH bridge and the water molecule were optimized, given that very small variations in the geometry (such as those induced by the packing forces in the crystal) can produce large changes in the calculated coupling constants, making the comparison with the experimental value meaningless.[41]

Acknowledgements

Work supported by Projects PGIDIT07PXIB209039PR and IN-CITE09E1R209058ES (Xunta de Galicia, Spain), PICT 2006-00439 (SECyT), PIP 112-2008-01-01079 (CONICET) and CAI+D 11-058 2009 (UNL) in Argentina. C. D. B is a member of CONICET (Argentina). C. N, A. M, R. B, J. L. and C. L thank the program "Joint Portuguese–Spanish Project 2007" for the bilateral agreement number 63/07(Portugal)/HP2006-0119 (Spain). C. N. thanks Fundação para a Ciência e a Tecnologia/FEDER (Portugal/EU) by the postdoctoral contract SFRH/BPD/65367/2009. J. L. C., C. L. and L. V. thank Xunta de Galicia for the Isidro Parga Pondal Research program. We acknowledge some of the MALDI-TOF-MS spectra to Dr Luz Fernandes from REQUIMTE, University NOVA de Lisboa.

References

1 (*a*) I. M. Wasser, S. de Vries, P. Moenne-Loccoz, I. Schroder and K. D. Karlin, *Chem. Rev.*, 2002, **102**, 1201; (*b*) G. Parkin, *Chem. Rev.*, 2004, **104**, 699; (*c*) N. Mitic, S. J. Smith, A. Neves, L. W. Guddat, L. R. Gahan and G. Schenk, *Chem. Rev.*, 2006, **106**, 3338; (*d*) F. B. Johansson, A. D. Bond, U. G. Nielsen, M. Boujemaa;, K. S. Murray, K. J. Berry, J. A. Larrabee and C. J. McKenzie, *Inorg. Chem.*, 2008, **47**, 5079.
2 (*a*) L. M. Mirica, X. Ottenwaelder and T. D. P. Stack, *Chem. Rev.*, 2004, **104**, 1013; (*b*) E. I. Solomon, P. Chen, M. Metz, S.-K. Lee and A. E. Palmer, *Angew. Chem., Int. Ed.*, 2001, **40**, 4570; (*c*) K. D. Karlin, S. Kaderli and A. D. Zuberbühler, *Acc. Chem. Res.*, 1997, **30**, 139; (*d*) H. Decker, R. Dillinger and F. Tuczek, *Angew. Chem., Int. Ed.*, 2000, **39**, 1591; (*e*) T. Lind and P. E. M. Siegbahn, *J. Phys. Chem. B.*, 1999, **103**, 1193; (*f*) H. Decker, T. Schweikardt and F. Tuczek, *Angew. Chem., Int. Ed.*, 2006, **45**, 4546; (*g*) P. E. M. Siegbahn, *J. Biol. Inorg. Chem.*, 2003, **8**, 567; (*h*) E. A. Lewis and W. B. Tolman, *Chem. Rev.*, 2004, **104**, 1047.
3 K. A. Magnus, H. Ton-That and J. E. Carpenter, *Chem. Rev.*, 1994, **94**, 727.
4 T. Klabunde, C. Eicken, J. Sacchettini and B. Krebs, *Nat. Struct. Biol.*, 1998, **5**, 1084.
5 C. Gerdemann, C. Eicken and B. Krebs, *Acc. Chem. Res.*, 2002, **35**, 183.
6 (*a*) C. Eicken, F. Zippela, K. Büldt-Karentzopoulosab and B. Krebs, *FEBS Lett.*, 1998, **436**, 293.
7 Y. Matoba, T. Kumagai, A. Yamamoto, H. Yoshitsu and M. Sugiyama, *J. Biol. Chem.*, 2006, **281**, 8981.
8 (*a*) N. Sin, L. Meng, M. Q. W. Wang, J. J. Wen, W. G. Bornmann and C. M. Crews, *Proc. Natl. Acad. Sci. U. S. A.*, 1997, **94**, 6099; (*b*) S. Liu, J. Widom, C. W. Kemp, C. M. Crews and J. Clardy, *Science*, 1998, **282**, 1324.
9 S. L. Roderick and B. W. Matthews, *Biochemistry*, 1993, **32**, 3907.

10 D. E. Wilcox, *Chem. Rev.*, 1996, **96**, 2435.
11 N. Sträter, W. N. Lipscomb, T. Klabunde and B. Krebs, *Angew. Chem.*, 1996, **108**, 2158, (*Angew. Chem., Int. Ed. Engl.*, 1996, **35**, 2024).
12 N. C. Horton and J. J. Perona, *Nat. Struct. Biol.*, 2001, **8**, 290.
13 (*a*) C.-G. Zhan, O. N. de Souza, R. Rittenhouse and R. L. Ornstein, *J. Am. Chem. Soc.*, 1999, **121**, 7279; (*b*) S. K. Smoukov, L. Quaroni, X. Wang, P. E. Doan, B. M. Hoffman and L. Que, Jr., *J. Am. Chem. Soc.*, 2002, **124**, 2595.
14 (*a*) A. Banerjee, S. Sarkar, D. Chopra, E. Colacio and K. K. Rajak, *Inorg. Chem.*, 2008, **47**, 4023; (*b*) B. Bauer-Siebenlist, F. Meyer, E. Farkas, D. Vidovic and S. Sebastian Dechert, *Chem.–Eur. J.*, 2005, **11**, 4349.
15 R. H. Holm and E. I. Solomon, *Chem. Rev.*, 2004, **104**, 347 (guest ed.) and references cited therein.
16 (*a*) C. Núñez, E. Oliveira, L. Giestas, L. Valencia, A. Macías, J. C. Lima, R. Bastida and C. Lodeiro, *Inorg. Chim. Acta*, 2008, **361**, 2183; (*b*) C. Nuñez, R. Bastida, A. Macías, C. Lodeiro and L. Valencia, *Inorg. Chim. Acta*, 2009, **362**, 3454; (*c*) C. Núñez, R. Bastida, A. Macías, E. Bértolo, L. Fernandes, J. L. Capelo and C. Lodeiro, *Tetrahedron*, 2009, **65**, 6179; (*d*) C. Núñez, R. Bastida, A. Macías, A. Aldrey and L. Valencia, *Polyhedron*, 2010, **29**, 126.
17 (*a*) A. Tamayo, J. Casabo, L. Escriche, C. Lodeiro, B. Covelo, C. D. Brondino, R. Kivekäs and R. Sillampää, *Inorg. Chem.*, 2006, **45**, 1140; (*b*) A. Tamayo, L. Escriche, C. Lodeiro, J. Ribas-Ariño, R. Ribas, B. Covelo and J. Casabo, *Inorg. Chem.*, 2006, **45**, 7621.
18 C. Nuñez, R. Bastida, A. Macías, L. Valencia, J. Ribas, J. L. Capelo and C. Lodeiro, *Dalton Trans.*, 2010, **39**, 7673.
19 (*a*) N. S. Grill, R. H. Nuttall, D. E. Scaife and D. W. Sharp, *J. Inorg. Nucl. Chem.*, 1961, **18**, 79; (*b*) S. Aime, M. Botta, U. Casellato, S. Tamburini and P. A. Vigato, *Inorg. Chem.*, 1995, **34**, 5825.
20 (*a*) A. S. Quist, J. B. Bates and G. E. Boyd, *J. Chem. Phys.*, 1971, **54**, 4896; (*b*) O. L. Casagrande and A. E. Mauro, *Polyhedron*, 1997, **16**, 2193.
21 P. Guerriero, U. Casellato, S. Tamburini, P. A. Vigato and R. Graziani, *Inorg. Chim. Acta*, 1987, **129**, 127.
22 A. K. Livesey and J. C. Brochon, *Biophys. J.*, 1987, **52**, 693.
23 E. Pretsch, T. Clerc, J. Seibl, W. Simon, *Tables of Spectral Data for Structure Determination of Organic Compounds*, 2nd ed., Springer, 1989.
24 A. B. P. Lever, *Inorganic Electronic Spectroscopy,* 2nd ed., Elsevier, 1984.
25 L. Fernandes, M. Boucher, J. Fernández-Lodeiro, E. Oliveira, C. Nuñez, H. M. Santos, J. L. Capelo, O. Nieto-Faza, E. Bértolo and C. Lodeiro, *Inorg. Chem. Commun.*, 2009, **12**, 905.
26 U. Bossek, D. Nühlen, E. Bill, T. Glaser, C. Krebs, T. Weyhermüller, K. Wieghardt, M. Lengen and A. X. Trautwein, *Inorg. Chem.*, 1997, **36**, 2834.
27 (*a*) D. A. Brown, W. K. Glass, N. J. Fitzpatrick, T. J. Kemp, W. Errington, G. J. Clarkson, W. Haase, F. Karsten and A. H. Mahdy, *Inorg. Chim. Acta*, 2004, **357**, 1411; (*b*) Y. Dussart, C. Harding, P. Dalgaard, C. McKenzie, R. Kadirvelraj, V. McKee and J. Nelson, *J. Chem. Soc., Dalton Trans.*, 2002, 1704; (*c*) F. B. Johansson, A. D. Bond, U. G. Nielsen, B. Moubaraki, K. S. Murray, K. J. Berry, J. A. Larrabee and C. J. McKenzie, *Inorg. Chem.*, 2008, **47**, 5079; (*d*) D. Black, A. J. Blake, K. P. Dancey, A. Harrison, M. McPartlin, S. Parsons, P. A. Tasker, G. Whittaker and M. Schröder, *J. Chem. Soc., Dalton Trans.*, 1998, 3953; (*e*) F. P. Pruchnik, U. Dawid and A. Kochel, *Polyhedron*, 2006, **25**, 3647.
28 M. A. Hitchman, *Inorg. Chem.*, 1977, **16**, 1985.
29 A. Bencini, D. Gatteschi, *EPR of exchange coupled systems*, Springer Verlag, Berlin–Heidelberg, 1990.
30 T. D. Smith and J. R. Pilbrow, *Coord. Chem. Rev.*, 1974, **13**, 173.
31 (*a*) D. J. Hodgson, *Prog. Inorg. Chem.*, 1975, **19**, 173; (*b*) V. H. Crawford, H. W. Richardson, J. R. Wasson, D. J. Hodgson and W. E. Hatfield, *Inorg. Chem.*, 1976, **15**, 2107; (*c*) E. Ruiz, P. Alemany, S. Alvarez and J. Cano, *J. Am. Chem. Soc.*, 1997, **119**, 1297; (*d*) A. Rodriguez-Fortea, E. Ruiz, S. Alvarez and P. Alemany, *Dalton Trans.*, 2005, 2624; (*e*) H. Hu, Y. Liu, D. Zhang and C. Liu, *THEOCHEM*, 2001, **546**, 73.
32 (*a*) A. K. Patra, M. Ray and R. Mukherjee, *Polyhedron*, 2000, **19**, 1423; (*b*) 5. A. Koval, K. Schilden, A. M. Schuitema, P. Gamez, C. Belle, J. Pierre, M. Lüken, B. Krebs, O. Roubeau and J. Reedijk, *Inorg. Chem.*, 2005, **44**, 4372.
33 P. Chaudhuri, D. Ventur, K. Wieghardt, E. Peters, K. Peters and A. Simon, *Angew. Chem., Int. Ed. Engl.*, 1985, **24**, 57.
34 A. Rodríguez-Fortea, E. Ruiz, S. Alvarez and P. Alemany, *Dalton Trans.*, 2005, 2624.
35 M. W. A. Steenland, W. Lippens, G. G. Herman and A. M. Goeminne, *Bulletin des Sociétés Chimiques Belges*, 2010, **102**, 239.
36 G. M. Sheldrick, SADABS, Program for Empirical Absorption Correction of Area Detector Data, University of Göttingen, Germany, 1996.
37 SHELXTL version, An Integrated System for Solving and Refining Crystal Structures from Diffraction Data (Revision 5.1), Bruker AXS LTD.
38 O. Kahn, *Molecular Magnetism*, VCH Publishers Inc., New York, 1993.
39 (*a*) A. D. Becke, *J. Chem. Phys.*, 1993, **98**, 5648; (*b*) C. T. Lee, W. T. Yang and R. G. Parr, *Phys. Rev. B: Condens. Matter*, 1988, **37**, 785; (*c*) S. H. Vosko, L. Wilk and M. Nusair, *Can. J. Phys.*, 1980, **58**, 1200; (*d*) P. J. Stephens, F. J. Devlin, C. F. Chabalowski and M. J. Frisch, *J. Phys. Chem.*, 1994, **98**, 11623.
40 M. J. Frisch, G. W. Trucks, H. B. Schlegel, G. E. Scuseria, M. A. Robb, J. R. Cheeseman, V. G. Zakrzewski, J. A. Jr,. Montgomery, R. E. Stratmann, J. C. Burant, S. Dapprich, J. M. Millam, A. D. Daniels, K. N. Kudin, M. C. Strain, O. Farkas, J. Tomasi, V. Barone, M. Cossi, R. Cammi, B. Mennucci, C. Pomelli, C. Adamo, S. Clifford, J. Ochterski, G. A. Petersson, P. Y. Ayala, Q. Cui, K. Morokuma, D. K. Malick, D. A. Rabuck, K. Raghavachari, J. B. Foresman, J. Cioslowski, J. V. Ortiz, A. G. Baboul, B. B. Stefanov, G. Liu, A. Liashenko, P. Piskorz, I. Komaromi, R. Gomperts, R. L. Martin, D. J. Fox, T. Keith, M. A. Al-Laham, C. Y. Peng, A. Anayakkara, C. Gonzalez, M. Challacombe, P. M. W. Gill, B. Johnson, W. Chen, M. W. Wong, J. L. Andres, C. Gonzalez, M. Head-Gordon, E. S. Replogle, J. A. Pople, *Gaussian*, Inc.: Pittsburgh, PA, 2003.
41 E. Ruiz, J. Cano, S. Alvarez and P. Alemany, *J. Comput. Chem.*, 1999, **20**, 1391.